Journal of Electroceramics, 9, 199–207, 2002

P-Type Electronic Transport in $Ce_{0.8}Gd_{0.2}O_{2-\delta}$: The Effect of Transition Metal Oxide Sintering Aids

DUNCAN P. FAGG,* VLADISLAV V. KHARTON & JORGE R. FRADE
Department of Ceramics and Glass Engineering, CICECO, University of Aveiro, 3810-193 Aveiro, Portugal

Submitted August 10, 2002; Revised December 23, 2002; Accepted January 6, 2003

Abstract. Small (2 mol%) additions of cobalt, iron and copper oxides into $Ce_{0.8}Gd_{0.2}O_{2-\delta}$ considerably improve sinterability of ceria-gadolinia (CGO) solid electrolyte, making it possible to obtain ceramics with 95–99% density and sub-micron grain sizes at 1170–1370 K. The minor dopant additions have no essential effect on the total and ionic conductivity, whilst the *p*-type conduction in the transition metal-containing materials at 900–1200 K is 8–30 times higher than that in pure CGO. The oxygen ion transference numbers of the Co-, Fe- and Cu-doped ceramics, determined by the modified e.m.f. technique under oxygen/air gradient, are in the range 0.89–0.99. The electron-hole contribution to the total conductivity increases with temperature, as the activation energy for ionic conduction, 78 to 82 kJ/mol, is significantly lower than that for the *p*-type electronic transport (139–146 kJ/mol). The results show that CGO sintered with such additions can still be used as solid electrolytes for intermediate-temperature electrochemical applications, including solid oxide fuel cells (SOFCs) operating at 770–970 K, but that increasing operation temperature is undesirable due to performance loss.

Keywords: gadolinia-doped ceria, solid electrolyte, sintering aid, transference number, hole conductivity

1. Introduction

Solid electrolytes based on doped cerium dioxide, $Ce(R)O_{2-\delta}$ (R: rare earth cations), are considered to be one of the most promising alternatives to yttria-stabilized zirconia (YSZ) ceramics for applications in electrochemical devices operating at intermediate temperatures (770–970 K), as the ionic conductivity of ceria-based materials in this temperature range is 4 to 5 times higher [1–7]. At temperatures below 1000 K electronic leakage due to reduction of Ce^{4+} to Ce^{3+} has been shown to be minimal and successful incorporation in devices such as solid oxide fuel cells (SOFCs) has been demonstrated. The wide use of ceria-based electrolytes is hindered, however, by poor mechanical strength, a problem notably undesirable for electrolyte-supported cells. The achievement of sufficient density by conventional sintering methods requires high temperatures (up to 1770–1870 K) resulting in the formation of microstructures with grain sizes in the micron range which subsequently offer poor mechanical stability [7, 8]. Recently, Kleinlogel and Gauckler [6, 7] have sintered dense Gd-substituted CeO_2 (CGO) with nanosized grains at temperatures as low as 1170 K by the addition of small quantities (<5 mol%) of binary transition metal oxides such as cobalt or copper oxide. The nanosized grain structure is likely to have greater mechanical stability than conventionally processed CGO sintered at higher temperatures.

Doping with trace amounts of transition metal oxides and fabrication of nanocrystalline CGO ceramics may be advantageous since a greater oxygen exchange rate can be achieved due to higher electronic conductivity at the electrolyte surface [4, 9–11]. For example, incorporation of transition metal cations into the surface layers of YSZ ceramics was shown to considerably decrease the electrode polarization [12, 13]. A similar effect was observed for 2% Pr-doped CGO, where the variable-valence praseodymium cations simultaneously increase electron-hole transport and act as catalytically-active centres [14].

*To whom all correspondence should be addressed. Email: duncan@cv.ua.pt

Conversely, higher electronic conduction resulting from both doping and nano-scale grain size may have a negative effect on the electrochemical cell performance. Though results on the total conductivity of 2%Co-doped CGO as a function of oxygen partial pressure indicated that the both ionic conductivity and electrolytic domain at low $p(O_2)$ are essentially unaffected by the doping [7], total conductivity measurements are usually insufficient for a definite conclusion on the electronic contribution to the total conductivity, when predominantly ionic. Nanocrystalline ceria is well known to exhibit a greater electronic transport than that in the materials consisting of micron-scale grains [4, 9]. In addition, comparison of results on the conductivity of Cu- and Co-containing CGO [6, 7] with data on solid electrolytes of stabilized ZrO_2 and Bi_2O_3, co-doped with rare-earth and transition metal cations [10, 15], may suggest an increase in the *p*-type conductivity of the doped ceria at temperatures below 970 K.

Continuing our research on CeO_2-based solid electrolytes [14, 16–19], the present work is focused on the study of minor electron-hole contributions to the total conductivity of CGO ceramics with sub-micron grain size, prepared using 2 mol% additions of the sintering aids: Co, Cu and Fe oxides. Results are presented on the shrinkage, microstructure, total conductivity and oxygen-ion transference numbers of sintered materials in oxidizing conditions. These data are compared with the corresponding quantities for $Ce_{0.80}Gd_{0.20}O_{2-\delta}$ and $Ce_{0.80}Gd_{0.18}Pr_{0.02}O_{2-\delta}$ ceramics, published earlier [17].

2. Experimental

Commercial $Ce_{0.80}Gd_{0.20}O_{2-\delta}$ powder (Rhodia GmbH, FRG) with average crystallite size of 20 nm and specific surface area of about 26 m^2/g was used as starting material to which 2 mol% metal oxide was added in the form of nitrate, $Fe(NO_3)_3{\cdot}9H_2O$, $Co(NO_3)_2{\cdot}6H_2O$ (Merck KGaA, FRG), or $Cu(NO_3)_2{\cdot}2.5H_2O$ (RdH GmbH, FRG). For comparison, a series of CGO samples doped with 2 mol% praseodymium oxide were prepared by a similar technique using $Pr(NO_3)_3{\cdot}5H_2O$ (RdH GmbH). Note that the starting $Ce_{0.80}Gd_{0.20}O_{2-\delta}$ powder, used in this work, is the same as that used by Kleinlogel and Gauckler [6, 7], who also employed the nitrate method to introduce transition metal dopants into the ceria solid electrolyte.

Stoichiometric amount of an aqueous solution of the dopant nitrate was added to the CGO powder and well mixed. After drying, the powder was milled in an agate mortar and dry pressed into pellets (diameter of 20 mm, pressure of about 30 MPa) followed by isostatic pressing at 200 MPa. Sintering behavior was studied using a Linseis dilatometer on rectangular green compacts ($0.6 \times 0.5 \times 0.5$ cm^3) with a constant heating rate of 5 K/min was used. A second batch of samples were identically prepared and analyzed in the dilatometer to follow sintering behavior with time. A heating rate of 10 K/min was used to achieve the temperature of maximum sintering rate specific for each metal oxide dopant, as located by the first dilatometric experiment. Dwell time at this specific temperature was 12 hours. Further samples were made for microstructural and electrical characterization by sintering in air at temperatures corresponding to maximum shrinkage rate during 5 hours; the heating/cooling rates were 10 K/min. The final density of sintered ceramic materials was determined by the Archimedes method.

Hereafter the compositions are designated as 2%M-CGO, where M denotes the transition metal oxide. Overall phase composition was determined by X-ray diffraction (XRD) using a Rigaku Geigerflex diffractometer (Cu K_α radiation); the unit cell parameters were calculated with the program FULLPROF. No evidence of secondary phases was discernible by XRD. Transmission electron microscopy (TEM) coupled with energy dispersive analysis (EDS), performed using a Hitachi H9000-NA instrument, was used to follow microstructural and area-specific compositional variations. For TEM/EDS, samples were supported on either copper or nickel formvar grids, dependant of composition, by immersion in suspensions of crushed samples in absolute ethanol. When possible, microstructural analysis was also performed by scanning electron microscopy (SEM) on ceramic samples, polished and then thermally etched for 30 min at temperatures 100 K below that of the respective sintering temperature. Electrical characterization was performed on dense pellets using the 4- and 2-point a.c. impedance methods. Bulk and grain boundary contributions to total conductivity were separated by fitting using the Equivalent Circuit program. Trace electron-hole conductivity was separated from total electrical conductivity using the modified e.m.f. method first proposed by Gorelov [20]. This modification of the classical e.m.f. technique, based on determination of the open-circuit voltage of oxygen

concentration cells, increases measurement sensitivity and eliminates possible errors in the determination of ion transference numbers arising due to electrode polarization, errors that are shown to be non-negligible for electrolyte-type materials which possess relatively minor electronic conductivity [17, 21]. The experimental set-up, measurement procedure and also comparison of this technique with the traditional approach are well documented in the literature [17, 21].

3. Results and Discussion

3.1. Sintering

Figure 1 shows the sintering behavior of CGO doped with 2% cobalt, copper, iron and praseodymium oxides; the linear shrinkage rate [$d(\Delta L/L_0)/dT$] is plotted as a function of temperature. As previously reported by Kleinlogel and Gauckler [6, 7], transition metal oxide additions are highly efficient as sintering aids for ceria-based materials, promoting an increase in the maximum shrinkage rate and also shifting the specific temperatures of maximum shrinkage rate with respect to that of the undoped material. In the 2%Co-CGO and 2%Cu-CGO cases these shifts are towards lower temperature whilst for 2%Fe-CGO a shift to higher temperature is observed (Fig. 1 and Table 1). The width of the shrinkage temperature range also decreases and for Co-, Cu- and Fe-containing materials is significantly narrower, characteristic of a liquid phase-assisted sintering [22]. The addition of praseodymium oxide shifts the temperature of maximum shrinkage rate to lower temperature, but does not assist sintering behavior in the same way as do the transition metal oxides, instead a lower shrinkage rate than that of the undoped material is observed.

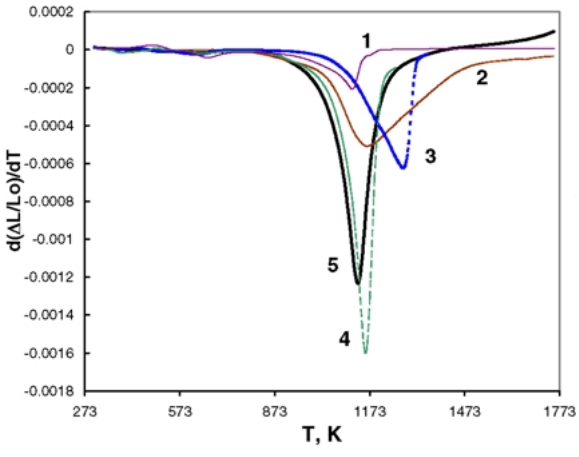

Fig. 1. Temperature dependence of the linear shrinkage rate for (1) 2%Pr-CGO, (3) pure CGO ($Ce_{0.8}Gd_{0.2}O_{2-\delta}$), (3) 2%Fe-CGO, (4) 2%Cu-CGO, and (5) 2%Ce-CGO.

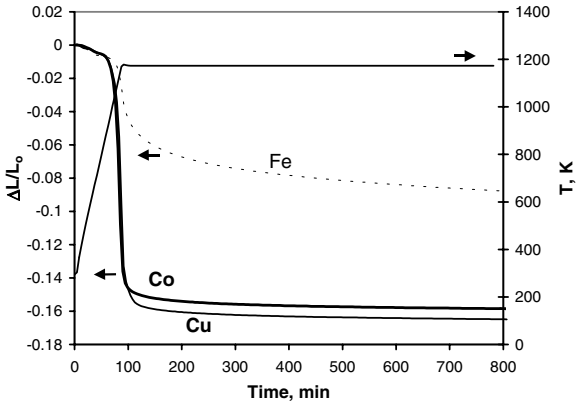

Fig. 2. Linear shrinkage as a function of time and temperature for 2%Co, Cu and Fe-doped CGO green compact in air. Ramp rate is 10 K/min, until dwell at 1173 K.

Figure 2 presents the shrinkage as a function of sintering time for Co-, Cu- and Fe-doped compositions at the sintering temperature of 1173 K, which corresponds to the experimentally determined temperature of maximum shrinkage rate for the cobalt- and copper-containing materials. The sintering processes are completed very rapidly, finishing within the initial minutes of the dwell for 2%Cu-CGO and 2%Co-CGO. In the case of 2%Fe-CGO, the sintering rate is found to be lower, a reflection of the higher temperature of maximum shrinkage rate required for this composition. The density values of ceramics, sintered in different conditions, are listed in Table 1. For 2%Co-CGO a decrease in the density is observed at sintering temperatures higher than 1373 K; this phenomenon is thought to possibly correspond to oxygen loss due to the reduction of Co cations at elevated temperatures and to a change in the sintering mechanism [7]. Such an assumption is supported by cobalt segregation with grain growth [23].

3.2. Microstructure

Representative examples of SEM and TEM micrographs of 2%Co-CGO, 2%Cu-CGO and 2%Fe-CGO

Table 1. Grain size and relative density of CeO_2-based ceramics sintered in various conditions.

Material	Sintering temperature (K)	Sintering time (h)	Relative density (%)	Grain size (μm)	Temperature of maximum shrinkage rate (K)
2%Co-CGO	1173	0.3	88.7 ± 0.4	0.1–0.2	1143
	1173	2	95.6 ± 0.5	0.1–0.2	
	1173	5	94.8 ± 0.6	0.1–0.2	
	1173	12	94.6 ± 0.5	0.1–0.2	
	1273	5	99.5 ± 0.2		
	1373	5	99.4 ± 0.3	0.3–0.5	
	1573	5	95.0 ± 0.6		
	1773	5	83.4 ± 0.7	4–10	
2%Cu-CGO	1173	5	99.4 ± 0.4	0.3–0.4	1163
	1173	12	99.7 ± 0.3	0.3–0.4	
	1273	5	99.8 ± 0.3		
	1373	5	94.0 ± 0.6		
2%Fe-CGO	1173	5	72.5 ± 0.6		1288
	1173	12	74.5 ± 0.5		
	1273	5	98.8 ± 0.3	0.07–0.15	
	1373	5	99.3 ± 0.3	0.15–0.25	
CGO	1873	6	96.4 ± 0.5	1–8	
$Ce_{0.80}Gd_{0.18}Pr_{0.02}O_{2-\delta}$	1873	6	95.1 ± 0.8	2–10	

ceramics, sintered at the respective temperatures of maximum shrinkage rate, are given in Fig. 3. For 2%Co-CGO ceramics sintered at 1173 K, the average grain size is in the range of 100–200 nm, with no significant change in microstructure with increased sintering time. Under the same conditions the grains of 2%Cu-CGO are larger (300–400 nm), whilst for 2%Fe-CGO sintered at 1273 K this range is 70–150 nm. The average grain size at the respective temperatures of maximum shrinkage rate, therefore, decreases in the sequence Cu > Co > Fe, which correlates with the observed decrease in the maximum rate of shrinkage (Fig. 1). When sintering temperature of transition metal-containing CGO increases, the grains grow up to 4–10 μm (Table 1), similar to that in $Ce_{0.80}Gd_{0.20}O_{2-\delta}$ and $Ce_{0.80}Gd_{0.18}Pr_{0.02}O_{2-\delta}$ sintered at 1873 K [17]. Thus, dense CGO ceramics with sub-micron grain size can be obtained at 1140–1290 K.

It should be mentioned that the results on sintering and microstructure of ceria-based ceramics, doped with 2% transition metal oxides, both agree with and expand upon the observations presented by Kleinlogel and Gaukler [6, 7], as expected from the similar starting materials and preparation route. This uniformity ensures that the observed enhancement of the *p*-type electronic conductivity for 2%M-CGO ceramics, discussed below, is common for the nanocrystalline CGO obtained using these additions.

To assess compositional variations between bulk and grain boundary regions, TEM/EDS studies were performed. For the ceramics with sub-micron grains, accurate determination of grain boundary composition by EDS is beyond the instrumental resolution as typical boundary thicknesses are in the order of a few nanometers. To assist analysis, therefore, triple point regions were investigated, although the results can still only yield composition averaged over an area, which includes the triple point, some bulk material and perhaps also underlying grains. However, consistent variation between the average composition measured across a triple point and that measured for the grain for multiple analyses still yield useful information. Typical results are presented in Fig. 4 for the 2%Cu-CGO ceramics sintered at the respective temperature of maximum shrinkage rate. The concentration of the transition metal at the triple point regions is observed to be clearly higher than that in the bulk. Similar results were obtained for the nanocrystalline 2%Co-CGO samples. This suggests that in the boundary layers of CGO grains the concentration of the transition element is greater and that complete incorporation of the transition metal additive into the bulk has not occurred.

3.3. Total Conductivity

Figure 5 shows a typical impedance spectrum measured at low temperature. Three distinct contributions

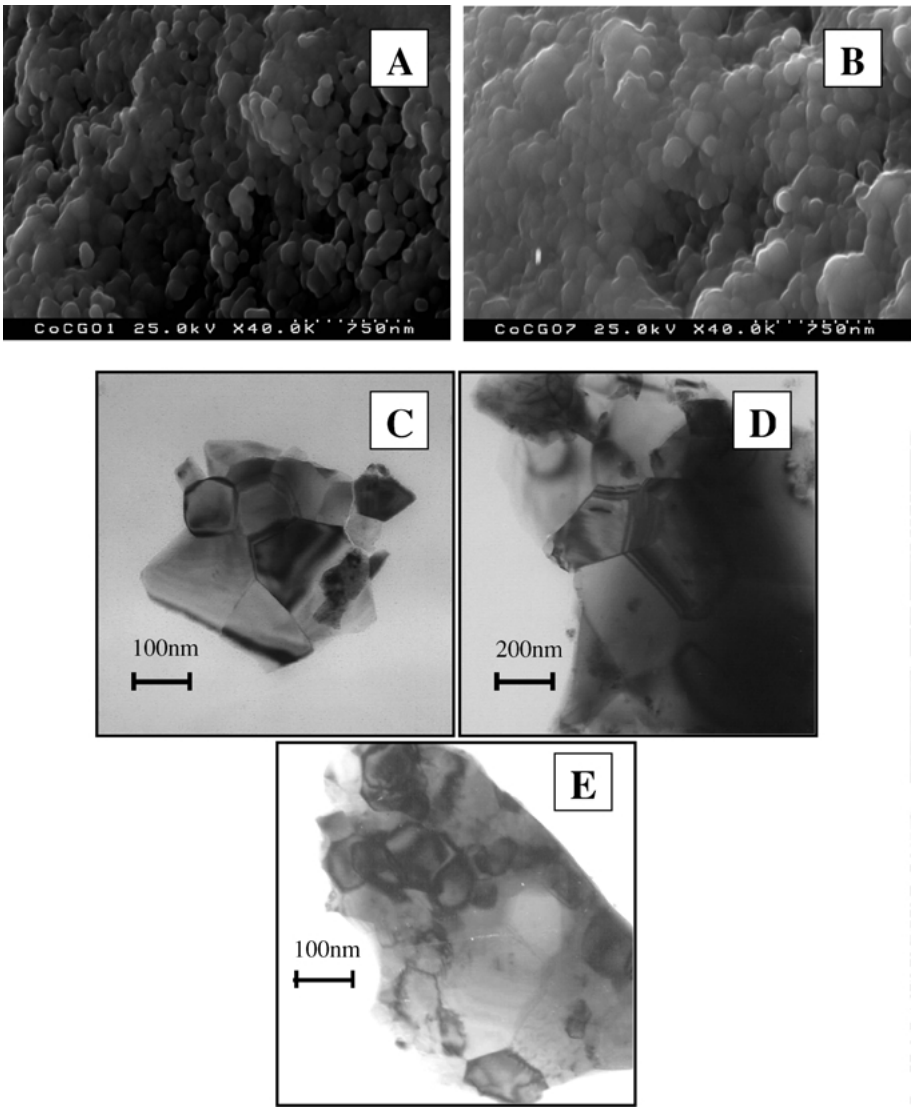

Fig. 3. SEM (A and B) and TEM (C, D and E) micrographs of 2%Co-CGO sintered at 1173 K for 20 min (A), 2%Co-CGO sintered at 1173 K for 2 h (B), 2%Co-CGO sintered at 1173 K for 5 h (C), 2%Cu-CGO sintered at 1173 K for 5 h (D), and 2%Fe-CGO sintered at 1273 K for 5 h (E).

can be observed with capacitance values characteristic of bulk, grain boundary and electrode processes. For the low temperature range, Fig. 6 shows the high frequency bulk and intermediate frequency grain boundary contributions to total conductivity for 2%Co-CGO sintered for different time periods at 1173 K. Due to the similar grain sizes of the samples, comparison of the grain boundary conductivity is performed using the total sample geometry. The bulk conductivity is essentially independent of sintering time, whilst the intermediate frequency grain boundary component is observed to be lower for the short sintering time of 20 minutes. This result may be considered to contradict the data of Kleinlogel and Gaukler [7], who suggested from low temperature total conductivity measurements, that higher grain boundary conductivities would be expected in compositions sintered for short time periods due to an amorphous grain-boundary layer of cobalt

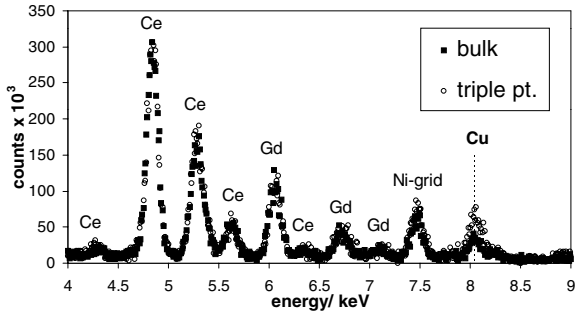

Fig. 4. TEM/EDS spectra of 2%Cu-CGO ceramics sintered at 1173 K for 5 h. The peak marked as "Ni-grid" is due to sample support.

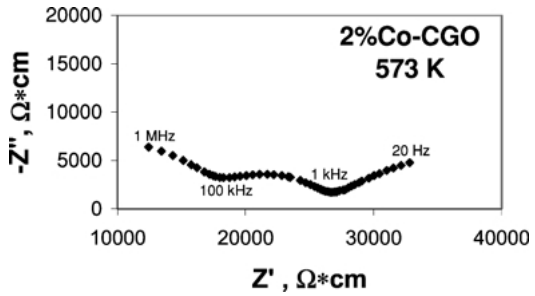

Fig. 5. Typical AC impedance spectrum of 2%Co-CGO ceramics sintered at 1173 K, measured at 573 K.

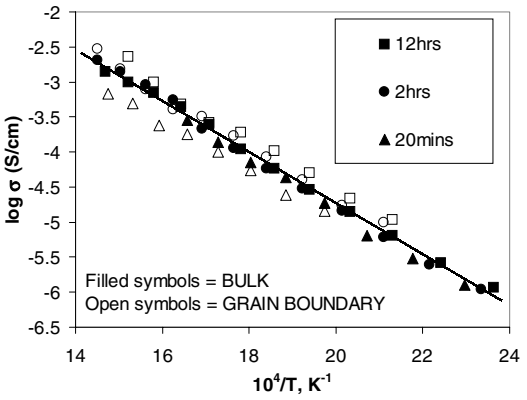

Fig. 6. Temperature dependence of bulk and grain boundary contributions to total conductivity in air, separated by a.c. impedance spectroscopy, for 2%Co-CGO sintered at 1173 K for different time periods and rapidly cooled.

oxide, a layer observed by TEM analysis to have had a width of approximately 2 nm. No cooling profile was stated in [7] but it is possible that those samples were quenched from the sintering temperature. In our experiment the samples were rapidly cooled but not quenched and in TEM analysis the presence of such amorphous grain boundary layers could not be observed. The most likely hypothesis is that, despite a short sintering time of 20 minutes in our experiments, enough time has elapsed on cooling that incorporation of the cobalt oxide in the surface layers of CGO grains is already complete. The apparent lower grain boundary conductivity observed, therefore, only results from the differing densities of these samples, (Table 1). The lower density of the sample sintered for 20 minutes leads to a non-resolvable intermediate frequency contribution which is in addition to that of the true grain boundary contribution. Such an assumption is in agreement with the observation that all grain boundary conductivities exhibit similar activation energies suggesting similar conduction mechanisms (Fig. 6).

Figure 7 compares the values of the total (bulk + grain boundary) conductivity of Co- Fe- and Cu-containing materials with that of undoped CGO ceramics, measured at temperatures above 900 K when the bulk and grain boundary contributions are indistinguishable. No significant difference in the conductivity is observed for the Co-, Cu- or Fe-doped samples sintered at 1173–1273 K with respect to pure CGO.

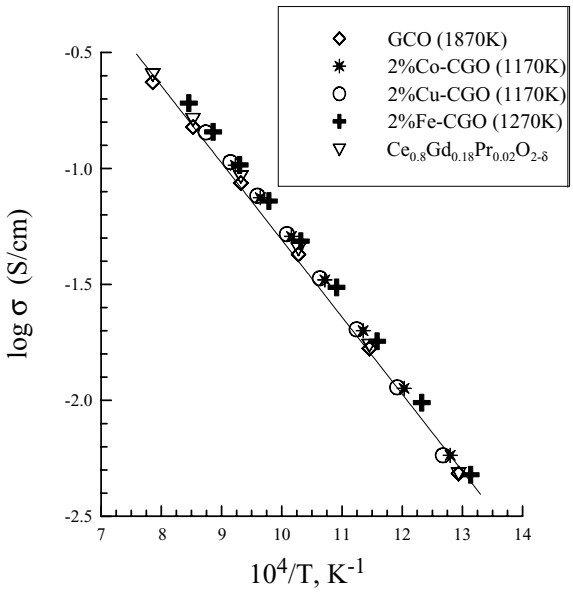

Fig. 7. Comparison of the total bulk conductivity of CGO ceramics doped with 2 mol% of the transition metal oxides, sintered for 5 hours at different temperatures, in air.

Table 2. Oxygen ion transference numbers of CGO ceramics doped with 2% of transition metal oxides, sintered at different temperatures for 5 hours.

Dopant	Sintering temperature (K)	T, K 923	973	1023	1073	1123	1173
Co	1173	0.98	0.97	0.95	0.93	0.90	0.89
Cu	1173	0.98	0.97	0.96	0.94	0.92	0.89
Fe	1273	0.99	0.98	0.97	0.96	0.94	0.92

3.4. *Electron-Hole Conduction*

Selected results on the oxygen ion transference numbers (t_o), averaged in the $p(O_2)$ range from 21 to 101 kPa, are presented in Table 2. Decreasing temperature results in a smaller electron-hole contribution to the total conductivity, clearly indicating that the activation energy for the p-type conduction is higher than that for ionic transport. Combining transference numbers with the total conductivity (σ) values obtained by impedance spectroscopy at corresponding temperatures, Fig. 7, allows p-type electronic conductivities to be estimated as

$$\sigma_p = (1 - t_o)\sigma \tag{1}$$

In oxidizing conditions the n-type contribution is extremely small [1, 16, 18] and was thus neglected. The activation energy (E_a) for the partial ionic and p-type electronic conductivities, Table 3, was calculated by the standard Arrhenius equation

$$\sigma = \frac{A_0}{T}\exp\left[-\frac{E_a}{\mathrm{RT}}\right] \tag{2}$$

where A_o is the pre-exponential factor.

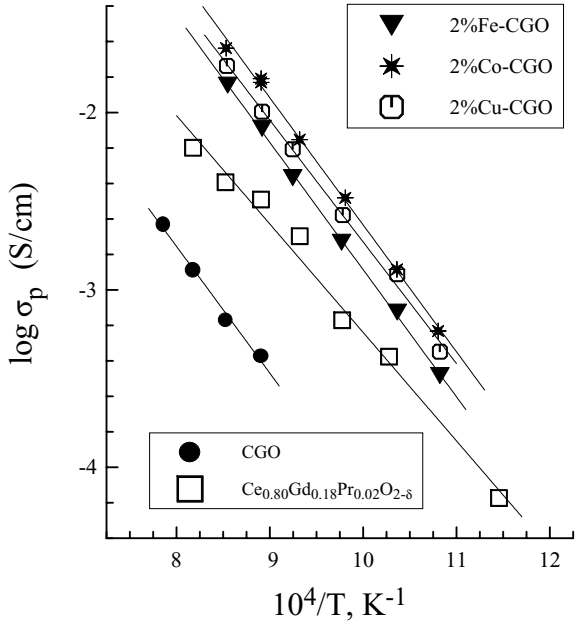

Fig. 8. Temperature dependence of the p-type electronic conductivity of CeO_2-based ceramics. All materials were sintered for 5 hours; the sintering temperature was 1173 K for the Co- and Cu-containing compositions and 1273 K for the Fe-doped material.

Figure 8 shows the p-type conductivity values of 2%M-CGO (M = Pr, Cu, Co, Fe) ceramics compared to that of the undoped CGO sintered at 1873 K. The presence of trace amounts of variable-valence dopants leads to an elevated p-type electronic transport in every case. For 2%Co-CGO sintered at 1173 K an enhancement of over 25 times is exhibited with respect to that of the pure gadolinia-doped ceria. Similar enhancements are observed for the Fe- and Cu-containing compositions. The electron-hole conductivity in $Ce_{0.80}Gd_{0.18}Pr_{0.02}O_{2-\delta}$,

Table 3. Regression parameters of the Arrhenius model for the partial ionic and p-type electronic conductivities of CeO_2-based ceramics in air.

Composition and sintering temperature	Conductivity	T, K	E_a (kJ/mol)	ln A_0 (S ∗ K/cm)
2%Co-CGO (1173 K)	Ionic	630–1090	79 ± 1	13.6 ± 0.2
	p-type electronic	920–1180	146 ± 3	18.4 ± 0.4
2%Cu-CGO (1173 K)	Ionic	540–1180	82.0 ± 0.9	13.9 ± 0.1
	p-type electronic	920–1170	139 ± 5	17.5 ± 0.5
2%Fe-CGO (1273 K)	Ionic	620–1180	78 ± 1	13.5 ± 0.2
	p-type electronic	920–1170	145 ± 3	17.8 ± 0.2
$Ce_{0.8}Gd_{0.2}O_{2-\delta}$	Ionic	720–1270	72.9 ± 0.8	12.7 ± 0.1
(1873 K)	p-type electronic	1070–1270	145 ± 8	14.8 ± 0.8
$Ce_{0.80}Gd_{0.18}Pr_{0.02}O_{2-\delta}$	Ionic	720–1270	74.0 ± 0.8	12.8 ± 0.1
(1873 K)	p-type electronic	870–1230	125 ± 6	14.6 ± 0.7

which is likely to be significantly contributed by Pr-enriched grain boundaries [14], has intermediate values between the undoped and transition metal-containing ceria ceramics.

All materials with sub-micron grains, sintered at 1173–1273 K, show similar σ_p values, slightly decreasing in the sequence Co ≥ Cu > Fe (Fig. 8). Activation energies for the *p*-type electronic transport are comparable both to each other and to that of pure CGO, varying in the narrow range 139 to 146 kJ/mol, which suggests a similar hole conduction mechanism. As no correlation between this behavior and the transport properties of binary transition-metal oxides [24] can be found, the enhanced *p*-type conductivity of doped CGO cannot be attributed to binary-oxide films at the grain boundaries. Furthermore, TEM/EDS analysis showed that, whilst the content of the transition metal additives in the grain bulk is dilute, their concentration in the grain boundary is considerably higher. Therefore, the relatively high electronic conductivity in CGO ceramics with sub-micron grains is thought to be due to the boundary layers of ceria grains, enriched with the variable-valence cations diffused in the course of sintering. Further significant contribution due to injection of *p*-type electronic charge carriers into the ceria grains may be expected [25].

In summary, although the oxygen ion transference numbers of Co-, Cu- and Fe-containing CGO ceramics are as low as 0.89–0.92 at 1173 K, the electron-hole contribution to the total conductivity decreases with reducing temperature. At 923 K the values of t_o are sufficiently high, varying in the range 0.97–0.99 (Table 2). Therefore, under the operation conditions of intermediate-temperature SOFCs (770–970 K) these materials can still be used as solid electrolytes, in agreement with the conclusions [6, 7]; further heating is undesirable due to larger performance losses.

4. Conclusions

The addition of 2 mol% transition metal oxides into $Ce_{0.8}Gd_{0.2}O_{2-\delta}$ ceramics considerably improves the sinterability of gadolinia-doped ceria. The maximum sintering rate is observed at 1120–1170 K for the Co- and Cu-doped materials, and around 1270 K for the Fe-containing composition. Annealing of such materials at 1170–1370 K allows nanocrystalline ceramics with 95–99% density to be obtained. Average grain size decreases in the sequence Cu > Co > Fe, analogous to the decrease in the maximum shrinkage rate. Further increase in sintering temperature results in grain growth up to the micron-scale level. If compared to pure CGO ceramics sintered at 1870 K having micron-sized grains, nanocrystalline CGO materials containing trace amounts of the transition metal oxides exhibit similar total conductivity values, but considerably higher *p*-type electronic transport. The oxygen ion transference numbers of the transition metal-containing materials sintered at 923–1273 K vary in the range from 0.89 to 0.99, decreasing when temperature increases. The observed behavior suggests that such materials can still be used as solid electrolytes for the intermediate-temperature SOFCs, but that the operation temperature should not exceed 1000 K.

Acknowledgments

This work was supported by the FCT, Portugal (PRAXIS and POCTI programs and the contract SFRH/BPD/3529/2000).

References

1. B.C.H. Steele, *Solid State Ionics*, **129**, 95 (2000).
2. J.P.P. Huijsmans, *Curr. Opin. Solid State Mat. Sci.*, **5**, 317 (2001).
3. O. Yamamoto, *Electrochim. Acta*, **45**, 2423 (2000).
4. H.L. Tuller, *Solid State Ionics*, **131**, 143 (2000).
5. S.J. Hong, K. Mehta, and A.V. Virkar, *J. Electrochem. Soc.*, **145**, 638 (1998).
6. C. Kleinlogel and L.J. Gaukler, in *SOFC VI*, edited by S.C. Singhal and M. Dokiya (The Electrochemical Society, Pennington, 1999), PV 99-19, p. 225.
7. C. Kleinlogel and L.J. Gauckler, *Solid State Ionics*, **135**, 567 (2000).
8. A. Atkinson and A. Selcuk, in *SOFC V*, edited by U. Stimming, S.C. Singhal, H. Tagawa, and W. Lehnert (The Electrochemical Society, Pennington, 1997), PV 97-40, p. 671.
9. Y.-M. Chiang, E.B. Lavik, I. Kosacki, H.L. Tuller, and J.Y. Ying, *J. Electroceramics*, **1**, 7 (1997).
10. V.V. Kharton, E.N. Naumovich, and A.A. Vecher, *J. Solid State Electrochem.*, **3**, 61 (1999).
11. B.C.H. Steele, K.M. Hori, and S. Uchino, *Solid State Ionics*, **135**, 445 (2000).
12. P. Bohac, A. Orliukas, and L. Gauckler, in *Proc. Int. Conf. "Electroceramics IV"*, edited by R. Waser (Augustinus Buchhandlung, Aachen, 1995), vol. 2, p. 771.
13. K.R. Thampi, A.J. McEvoy, and J. Van Herle, *J. Electrochem. Soc.*, **142**, 506 (1995).
14. V.V. Kharton, A.P. Viskup, F.M. Figueiredo, E.N. Naumovich, A.L. Shaulo, and F.M.B. Marques, *Mater. Lett.*, **53**, 160 (2002).

15. V.V. Kharton, E.N. Naumovich, and V.V. Samokhval, *Solid State Ionics*, **99**, 269 (1997).
16. V.V. Kharton, F.M. Figueiredo, L. Navarro, E.N. Naumovich, A.V. Kovalevsky, A.A. Yaremchenko, A.P. Viskup, A. Carneiro, F.M.B. Marques, and J.R.Frade, *J. Mater. Sci.*, **36**, 1105 (2001).
17. V.V. Kharton, A.P. Viskup, F.M. Figueiredo, E.N. Naumovich, A.A. Yaremchenko, and F.M.B. Marques, *Electrochim. Acta*, **46**, 2879 (2001).
18. L.M.Navarro, F.M.B.Marques, and J.R.Frade, *J. Electrochem. Soc.*, **144**, 267 (1997).
19. G.C. Mather, D.P. Fagg, A. Ringuedé, and J.R. Frade, *Fuel Cells*, **1**, 1 (2001).
20. V.P. Gorelov, *Elektrokhimiya*, **24**, 1380 (1988) (in Russian).
21. V.V. Kharton and F.M.B. Marques, *Solid State Ionics*, **140**, 381 (2001).
22. M.W. Barsoum, *Fundamentals of Ceramics* (McGraw-Hill Companies, Inc., New York, 1997).
23. D.P. Fagg, J.C.C. Abrantes, D. Pérez-Coll, P. Núñez, V.V. Kharton, and J.R. Frade, *Electrochim. Acta*, accepted for publication (2002).
24. P. Kofstad, *Nonstoichiometry, Diffusion and Electrical Conductivity in Binary Metal Oxides* (Wiley-Interscience, New York, 1972).
25. J.H. Kim and G.M. Choi, *Solid State Ionics*, **130**, 157 (2000).